



## Mechanically Induced Growth Rate Differential for Copper Layers Electroplated in Presence of Organic Additives

Bülent M. Başol,\* Ayşe Durmuş, Tony Wang, Serkan Erdemli, and Jeff Bogart

ASM NuTool Incorporated, Phoenix, Arizona 85034, USA

Electrochemical mechanical deposition (ECMD) planarizes copper films as they are plated on patterned wafer surfaces. The technique involves electrochemical deposition (ECD) and simultaneous sweeping of the cathode surface with a pad. Pad sweeping gives rise to a mechanically induced current suppression (MICS) phenomenon if plating is performed in electrolytes containing accelerator and suppressor additives as well as  $\text{Cl}^-$  ions. In this work we studied the MICS phenomenon by partially sweeping blanket wafer surfaces with a small pad and investigating effects of the bath chemistry and wafer surface derivatization on the copper growth rates at the swept and unswept regions of the surface. It was found that, at a given suppressor concentration, copper growth rate differential between the two regions was reduced with increasing accelerator concentration in the bath. Derivatization of the wafer surface in an accelerator-containing solution followed by ECMD in a suppressor-containing bath gave the largest growth differential between the swept and unswept surface portions, suggesting high planarization efficiency. Adsorption-desorption kinetics of the organic additives used in this work were obtained under ECD conditions and found to support the proposed mechanism of MICS.

© 2006 The Electrochemical Society. [DOI: 10.1149/1.2223993] All rights reserved.

Manuscript submitted January 5, 2006; revised manuscript received March 8, 2006. Available electronically July 26, 2006.

Electrochemically deposited (ECD) copper is the preferred material for the fabrication of advanced interconnect structures for integrated circuits because of copper's low resistivity and high electromigration resistance.<sup>1</sup> In a conventional interconnect fabrication process, copper is filled into and coated over the various size features formed in the dielectric layer deposited on the wafer surface. The plated copper film is then annealed and the excess material over the top surface or the field region of the wafer is removed by chemical mechanical polishing (CMP), electrochemical mechanical polishing (ECMP), or by a combination of both approaches leaving the conductors only within the cavities of the features.

In a typical ECD process, specially formulated electrolytes containing chloride ions and organic additives such as suppressors and accelerators are employed to achieve void-free superfilling or bottom-up filling of submicrometer-size high aspect ratio (AR) features.<sup>2-4</sup> This superfilling mechanism is not operative in large features with aspect ratios much smaller than 1.0. ECD coats such features in a conformal manner so that steps form over the large features, the step height being approximately equal to the depth of the features. The surface topography of a copper layer deposited on a patterned wafer surface by the standard ECD process, therefore, is nonplanar. The topography is planarized during the subsequent CMP step, which needs to planarize and remove copper without causing excessive dishing, erosion, or mechanical defects on the wafer. This task is becoming more and more challenging for the CMP process as mechanically weak low- $k$  materials are adapted as dielectric layers in advanced interconnect structures.

Electrochemical mechanical deposition (ECMD) process was developed to planarize the copper layer during the deposition step so that an already planarized film would be delivered to the CMP process.<sup>5-7</sup> Benefits of such planar copper layers for interconnect fabrication include less dishing, erosion, or metal loss.<sup>8-10</sup> Planarization during deposition would only be possible if copper deposited faster into the large cavities compared to the top surface of the wafer, i.e., if superfill is achieved into the low AR features. Because the well-known superfill mechanism for the high AR features, such as the curvature-enhanced accelerator coverage (CEAC) mechanism,<sup>4</sup> does not apply to filling low AR features, ECMD utilizes a newly identified mechanically induced superfilling (MISF) mechanism to achieve planarization of depositing copper over large features on the wafer surface.<sup>11</sup>

One mode of operation for ECMD involves sweeping the surface of the wafer with pad strips during copper electroplating. When the pad mechanical action is applied to the wafer surface during plating,

the deposition current density on the swept top surface is suppressed and deposition of copper into the wide features, which may have aspect ratios of smaller than 0.01, is enhanced.

The mechanism of MISF into the cavities and mechanically induced current suppression (MICS) at the swept surface of the wafer was recently studied and a model was proposed.<sup>11</sup> According to the proposed planarization model, the sweeping action of the pad induces a differential in the copper growth rates between the top surface of the wafer and the cavities by inducing a disparity in the surface coverage of active organic additives at the top surface and on the internal surfaces of the cavities. Figure 1a schematically shows a section of a patterned wafer surface with a cavity. The field region or the top surface is labeled as **F**, whereas the bottom surface of the cavity is labeled as **B**. Both the field region and the cavity internal surface are coated with a copper seed layer. During the ECMD process copper deposition is initiated while the pad starts to sweep the top surface **F** periodically. Therefore, region **F** becomes the swept region. The pad does not sag into the cavity, and therefore leaves the bottom surface **B** unswept. The average current density on the bottom surface **B** becomes larger than the average top surface current density because the sweeping action of the pad reduces the fractional surface coverage of the accelerator while increasing the fractional surface coverage of the suppressor at the swept region or the top surface.<sup>11</sup> Therefore, when the already-swept region enters into the plating solution and deposition starts, the effective surface coverage of the suppressor at that location is high. Accelerator then starts to readsorb on the top surface until the next pad sweep. The process continues in this cyclic fashion, resulting in planarization of

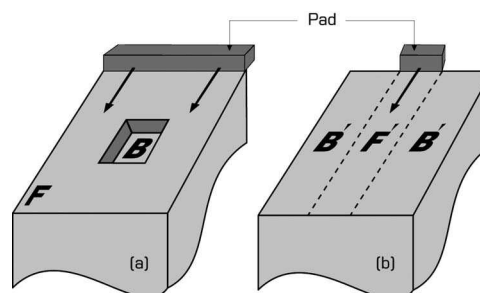


**Figure 1.** Schematic representation of ECMD process carried out (a) on a patterned substrate with a cavity where the pad sweeps the whole top surface; (b) on a flat substrate where a small pad sweeps only a portion of the surface.

\* Electrochemical Society Active Member.

the deposited layer. Dependence of the ECMD planarization efficiency on various experimental parameters, such as additive compositions and concentrations in the electrolyte, plating bath acidity, and derivatization of the wafer surface before the ECMD process, was previously studied using patterned wafers, copper sulfate-based electrolytes, and a single planarization pad strip.<sup>12</sup> It was determined that ECMD did not yield planarization in electrolytes free of organic additives or in solutions containing only  $\text{Cl}^-$  ions and accelerators. A low planarization efficiency of about 10–20% was measured in electrolytes containing  $\text{Cl}^-$  ions and suppressors. Only when  $\text{Cl}^-$  ions, accelerators, and suppressors were all present in the electrolyte, planarization efficiencies of about 60% were observed. When the wafer surface was derivatized in solutions comprising high accelerator concentration before the ECMD process, planarization efficiency of ECMD increased to 95%. Addition of levelers into the plating solution was found to be detrimental to planarization. High acid electrolyte (17 gm/L copper, 175 gm/L  $\text{H}_2\text{SO}_4$ ) provided higher planarization capability than low acid electrolyte (40 gm/L copper, 10 gm/L  $\text{H}_2\text{SO}_4$ ).

If the planarization mechanism of ECMD described above in reference to a patterned wafer surface (Fig. 1a) is correct, then a copper growth rate differential could also be induced on a blanket wafer surface if a small pad is used to sweep only a portion of the surface, leaving another portion unswept during copper plating. This is schematically shown in Fig. 1b, where an area of a blanket wafer surface is swept by a small pad piece in the direction of the arrow in a cyclic manner, forming on the surface a swept ring and an unswept region **B'**. The copper growth rate differential between the swept and unswept regions of a blanket wafer surface (Fig. 1b) and the copper growth rate differential between the top surface and the cavity region of a patterned wafer surface (Fig. 1a) should be directly related. In other words, a plating chemistry or a plating process condition that would yield high planarization efficiency for ECMD of a patterned wafer surface should also yield a high copper thickness differential between the swept and unswept regions of a blanket wafer surface. Therefore, we found that use of blanket wafers to study the MICS phenomenon, mechanism of ECMD, and optimization of ECMD planarization efficiency was much easier and economical than using patterned wafers.

We have recently carried out experiments where we swept a ring-shaped portion of a blanket wafer surface by a small pad during copper electroplating and studied the copper growth rate differential in the swept and unswept regions as a function of (i) the additives present in the plating bath, and (ii) the wafer rpm during deposition.<sup>13</sup> Results showed that there was no appreciable growth rate differential between the swept and unswept regions of the wafer if plating was carried out in an organic additive-free electrolyte or an electrolyte containing only accelerators and  $\text{Cl}^-$  ions. For electrolytes containing only  $\text{Cl}^-$  ions and suppressors a small differential was observed, whereas in an electrolyte containing both accelerators and suppressors in addition to  $\text{Cl}^-$  ions, the copper growth rate at the swept region was found to be appreciably lower than at the unswept region.<sup>13</sup> These results were in agreement with the findings of our prior work carried out on patterned wafers and summarized above.<sup>12</sup> The rpm dependence of the MICS phenomenon was modeled taking into account additive adsorption transients, and a good fit was obtained with the experimental results.<sup>13</sup> In the present work we carried out a more in-depth study of the MICS phenomenon by using blanket wafers and inducing copper growth rate differential on the wafer surface by partially sweeping the surface with a small pad. Copper thickness differential between the swept and unswept regions was investigated as a function of the concentrations of various additives in the plating electrolyte and preplating treatment of the wafer surface with organic additives. The findings of this study confirmed the validity of the previously proposed MICS mechanism and provided information about ways to improve the planarization efficiency of the ECMD process as applied to patterned wafer processing.

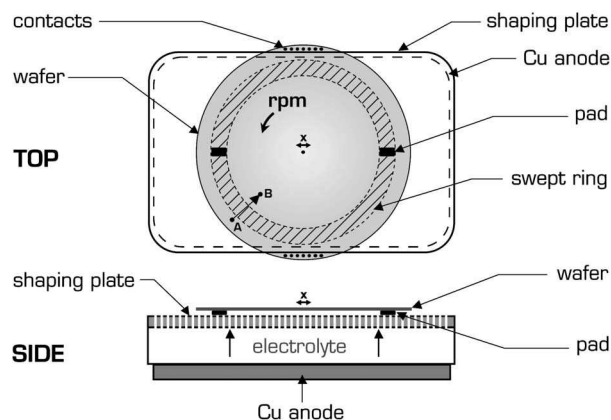


**Figure 2.** Top and side views of the experimental plating cell used to process 200 mm wafers in this work.

### Experimental

Schematic top and side views of the plating cell used in the experiments are shown in Fig. 2. The field-shaping plate is a porous rigid plate through which the plating solution rises up and reaches the wafer surface to be plated. The porosity on the shaping plate was designed to assure uniform film deposition. A rectangular copper anode was placed in a cavity under the shaping plate and two  $15 \times 10$  mm size pads were attached symmetrically along the  $x$  axis over the shaping plate at locations 70–85 mm from the center. The pads were made of a fixed-abrasive type material supplied by 3M Company and mounted on a spongy and soft backing.

Blanket wafers of 200 mm diameter with 300 Å thick Ta barrier film and 1000–1200 Å thick copper seed layer were used in this study. Wafers were lowered towards the shaping plate with a wafer holder (not shown) that could rotate as well as translate the wafer in the “ $x$ ” direction by controlled amounts and at controlled speeds. Multiple electrical contacts were made to the wafer surface at the two locations indicated in the figure. When the wafers were lowered down toward the shaping plate, wafer surface touched the plating solution and was pushed against the surface of the planarization pad pieces at a force level of about 0.8 psi. Plating was initiated 10 s after the wafer was immersed in the plating electrolyte and rotated as well as translated laterally by  $\pm 1$  mm at a speed of 1 mm/s. These motions continued during plating also. Rotation of the wafer and the physical contact with the two pad pieces generated a “swept ring” during the plating process as shown by the cross-hatched region in Fig. 2. A high acid copper sulfate electrolyte with 17 gm/L of copper, 175 gm/L of  $\text{H}_2\text{SO}_4$ , and 50 ppm of  $\text{Cl}^-$  was used for the plating work because previous work had shown a higher planarization efficiency for ECMD in high acid electrolyte compared to low acid electrolyte.<sup>12</sup> Cubath Viaform Suppressor and Cubath Viaform Accelerator available from ENTHONE were used as the organic additives. In an ECD process employing ENTHONE chemistry the typical accelerator and suppressor concentrations are 2–3 and 7–9 mL/L, respectively. These concentrations are used in the ECD process because they yield defect or void-free gap fill performance for submicrometer-size high AR vias and damascene structures on the wafer surface. Because ECMD process concerns itself with planarization of large features with extremely small ARs, additive concentrations for this application may be quite different. In this study one of our goals was to investigate the effect of additives on the MICS phenomenon, and therefore we have gone beyond the typical ECD concentration levels of these additives and varied the accelerator and suppressor concentrations in the 0–70 and 0–16 mL/L range, respectively. The average plating current density applied was 20 mA/cm<sup>2</sup>. After deposition, copper thickness profiles across the swept ring, such as from point A to point B in Fig. 2, were measured

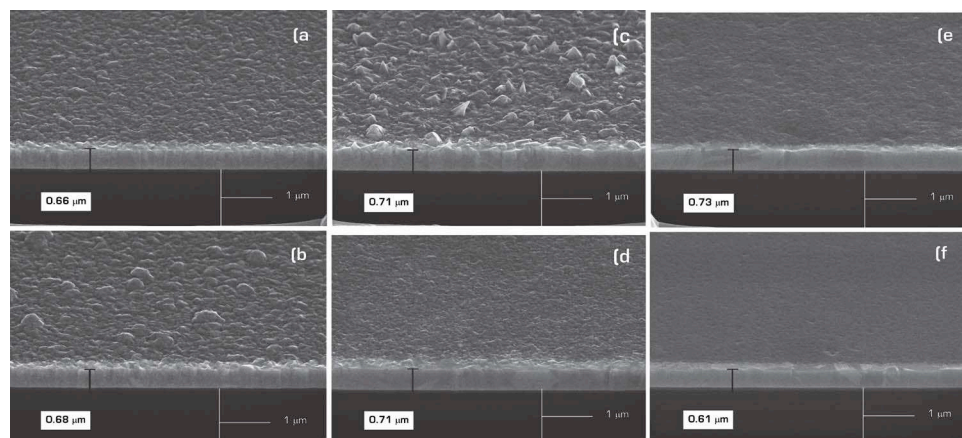


**Figure 3.** FIB/SEM micrographs taken from the unswept and swept regions of three wafers plated in electrolytes with various additive content; (a) unswept region plated in a bath with  $A = 2$  mL/L,  $S = 0$  mL/L; (b) swept region plated in a bath with  $A = 2$  mL/L,  $S = 0$  mL/L; (c) unswept region plated in a bath with  $A = 0$  mL/L,  $S = 8$  mL/L; (d) swept region plated in a bath with  $A = 0$  mL/L,  $S = 8$  mL/L; (e) unswept region plated in a bath with  $A = 2$  mL/L,  $S = 8$  mL/L; (f) swept region plated in a bath with  $A = 2$  mL/L,  $S = 8$  mL/L.

using a CDE RESMAP four-point probe station to determine any thickness differential between the swept and unswept sections of the wafer. Sheet resistance-to-thickness conversion was done using a resistivity value of  $2.5 \mu\Omega$  cm, which is the room temperature resistivity of our as-plated copper layers. Measurements were taken on at least four locations on the wafer. Variations in results were shown as error bars in the graphs. Dependence of the thickness differential on process variables such as concentrations of various organic additives in the plating bath was studied. Surface morphology of the copper film at the swept and unswept regions of the wafer was determined using an FEI Expida 1265 FIB/SEM system. Surface roughness was measured using a VEECO Dektak V300Si profiler. The presence of two small pads within the swept ring of the wafer introduces a certain amount of current shadowing in this region because the pads are insulating. This effect was calculated to be about 4% by taking the ratio of the total width of the two pads (2 cm) to the circumference ( $15.5 \pi$  cm) of a circle at the location of the center of the pads at 77.5 mm. Because the total plated copper thickness was about  $5000 \text{ \AA}$  in most of the experiments, the shadowing effect is expected to cause a step height of about  $200 \text{ \AA}$ . This amount was taken out of all experimental thickness differential data to leave only the electrochemical mechanical effect on the copper growth rate.

In a group of experiments, blanket wafers coated with barrier and seed layers were derivatized in accelerator containing deionized (DI) water for 30 s. Concentration of the accelerator in the water was 2 mL/L. After derivatization wafers were rinsed, dried, and used for copper plating in the cell of Fig. 2 within 10 min. The plating electrolyte in these experiments contained only 8 mL/L of suppressors and 50 ppm of  $\text{Cl}^-$  ions.

Polarization data were collected using an experimental plating cell consisting of a 100 mL beaker with about 5 cm diameter, a copper anode, and  $1 \times 2$  cm size wafer piece with copper seed layer that served as the cathode. Only 50 mL of solution was filled into the beaker to minimize solution volume. A constant current density of  $20 \text{ mA/cm}^2$  was applied between the anode and the cathode by a Princeton Applied Research (PAR-263A) potentiostat/galvanostat and the cathode voltage was monitored with respect to a calomel reference electrode as the additive content of the high acid electrolyte (with 50 ppm of  $\text{Cl}^-$ ) was manipulated during plating. The anode to cathode distance was 3 cm and the reference electrode was placed right next to the cathode. The solution was stirred rigorously in these experiments using a 2.5 cm long, 0.5 cm diameter magnetic rod rotating at 500 rpm to minimize the time for additive mixing into the solution. In one experiment suppressor and accelerator additives were introduced into the solution consecutively during plating at amounts of 8 and 2 mL/L, respectively, and the variation in cathode potential was recorded. Additives were introduced into the solution rapidly, using a dropper. In another experiment the cathode was introduced into a solution already containing 8 mL/L of sup-

pressors and 2 mL/L of accelerators and the transient of the cathode voltage was recorded. In a third experiment the copper seed surface was derivatized in a DI water solution with 2 mL/L of accelerators for 1 min. The sample was rinsed and dried and then used as a cathode for plating copper out of an electrolyte containing only 8 mL/L of suppressors. The voltage transient during deposition was recorded. In all of the above experiments the goal was to gather information about the kinetics of additive adsorption(desorption) on-(from) the wafer surface under ECD conditions.

## Results and Discussion

The focused ion beam-scanning electron microscope (FIB/SEM) cross sections of Fig. 3a-f were taken from the sections of copper layers within the swept and unswept regions of the wafer as a function of the organic additives present in the deposition electrolyte. Plating was carried out at 50 rpm and enough charge was deposited on the wafer for a  $5500 \text{ \AA}$  thick copper layer. Because the barrier and copper seed layer thicknesses were 300 and  $1100 \text{ \AA}$ , respectively, the FIB cross sections were expected to show a total film thickness of about  $0.69 \mu\text{m}$  over the dielectric layer, provided plating was perfectly uniform.

As can be seen from Fig. 3, the surface morphology of the films deposited out of an electrolyte containing only 2 mL/L of accelerator was relatively rough ( $\sim 100 \text{ \AA}$  surface roughness) with rounded features in the unswept (Fig. 3a) as well as swept (Fig. 3b) regions. In fact, roughness seemed to be larger in the swept region. The FIB cross sections showed a film thickness of about  $0.66\text{--}0.68 \mu\text{m}$  for both regions, suggesting that there was no measurable growth rate differential between the swept and unswept regions. For the film plated out of an electrolyte containing only 8 mL/L of suppressor, the unswept region (Fig. 3c) showed rough morphology ( $\sim 200 \text{ \AA}$ ) with nodules, whereas the swept region (Fig. 3d) was smooth with a roughness of about  $50 \text{ \AA}$ . Clearly, the mechanical action of the pad and the surfactant nature of the suppressor did not allow the nodule formation within the swept ring, although the average film thickness was still the same ( $\sim 0.71 \mu\text{m}$ ) in both regions within the accuracy of the measurement. Data in Fig. 3e and f were taken from the unswept and swept regions, respectively, of a wafer electroplated in an electrolyte containing 2 mL/L of accelerator and 8 mL/L of suppressor. In this case the copper film deposited on the unswept region under standard ECD conditions was smooth, with a roughness of about  $50 \text{ \AA}$  due to the leveling effect of the accelerator and suppressor additives, and the copper deposit within the swept ring had a mirror-finish surface with a roughness of  $20\text{--}30 \text{ \AA}$  due to both mechanical and chemical action of the ECMD process.<sup>14</sup> The copper layer of the swept region in this case was found to be at least  $0.1 \mu\text{m}$  thinner than the copper layer within the unswept region, suggesting that MICS mechanism was operative in the plating bath containing both suppressors and accelerators. Sheet resistance mea-

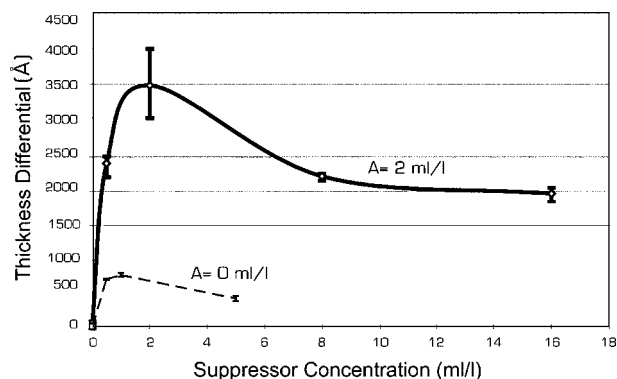


**Figure 4.** Copper thickness differential between the swept ring and unswept region of blanket wafers as a function of suppressor concentration in plating baths containing accelerators at concentrations of 0 and 2 mL/L.

measurements taken using a 4-point probe agreed well with the FIB data, confirming that we could use sheet resistance measurement in our study and that pad action in the swept ring did not change the resistivity of the as-deposited copper layers in any significant way. This is in agreement with the results of previous work on the comparative characterization of electrical and structural properties of copper layers deposited by the ECD and ECMD techniques.<sup>14</sup>

Figure 4 shows the experimentally determined dependence of the thickness differential on the suppressor concentration in two different plating baths, one without accelerators ( $A = 0$  mL/L) and the other with an accelerator concentration of  $A = 2$  mL/L. Depositions were carried out for 60 s at 80 rpm in these experiments. As stated before, in the absence of accelerators, a plating bath containing only suppressors yields a small thickness differential. This is shown by the data labeled “ $A = 0$ ” which also suggest that there is not a strong dependence of this small effect on the suppressor concentration. The second set of data for an accelerator concentration of 2 mL/L shows a sharp increase in the thickness differential when the suppressor concentration was increased first from zero to 0.5 mL/L and then to 2 mL/L. Further escalation of the suppressor concentration to 16 mL/L was found to saturate the thickness differential at a value of about 2000 Å. Considering the fact that the total plated copper thickness was about 5000 Å, this thickness differential represents about 40% reduction in the plating current density within the swept region of the wafer.

Figure 5 shows the variation of the measured thickness differential as a function of the accelerator content of the bath at a fixed suppressor concentration of 2 mL/L. For a suppressor concentration

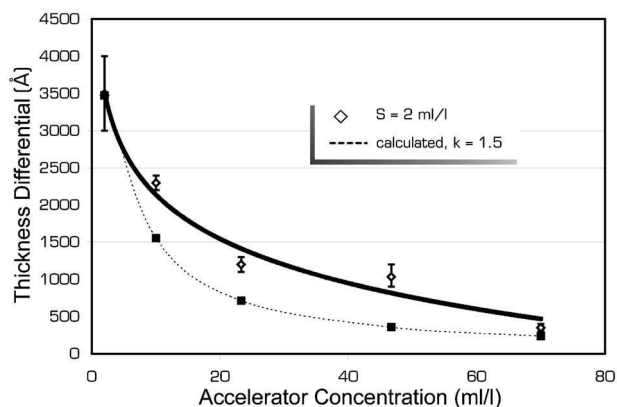


**Figure 5.** Experimentally determined and calculated copper thickness differential variations as a function of the accelerator concentration in an electrolyte with  $S = 2$  mL/L.

of 2 mL/L, the thickness differential was reduced appreciably and continuously as more and more accelerator was added to the chemistry. Similar behavior was observed when the experiment was repeated for a suppressor concentration of 0.5 mL/L. In this case the thickness differential declined to insignificant levels when accelerator concentration was increased to about 30 mL/L.

Assuming Tafel kinetics, the current density in the unswept region can be represented by

$$i_{\text{no pad}} = i_0(1 - \theta_{\text{no pad}})\exp[-\alpha_c FV/RT] \quad [1]$$

and the current density in the swept region can be given by<sup>13</sup>

$$\begin{aligned} i_{\text{pad}} &= i_0[1 - \theta_{\text{no pad}} - \theta_{\text{pad},0} \exp(-kt)]\exp[-\alpha_c FV/RT] \\ &= i_{\text{no pad}} - i_0\theta_{\text{pad},0} \exp(-kt)(-\alpha_c FV/RT) \end{aligned} \quad [2]$$

where  $i$  (mA/cm<sup>2</sup>) is a function of position and time,  $R$  is the gas constant (8.314 J mol K<sup>-1</sup>),  $F$  is the Faraday's constant (96,487 coulombs/mol),  $T$  is the temperature in Kelvin,  $\alpha_c$  is the transfer coefficient,  $\theta_{\text{no pad}}$  is the effective additive coverage in the unswept region,  $\theta_{\text{pad},0}$  is the additional additive coverage induced in the swept region due to the mechanical action right after a pad sweep, and  $k$  is the additive relaxation rate constant in s<sup>-1</sup>. The thickness differential,  $\Delta$ , which is the copper thickness difference between the unswept and swept regions right at the border between the two regions, can be derived from Eq. 1 and 2

$$\Delta = B \int i_0\theta_{\text{pad},0} \exp(-kt) dt = Bi_0\theta_{\text{pad},0}[1 - \exp(-kt_p)]/k \quad [3]$$

where  $t_p$  is the time period between pad sweeps,  $B$  is a proportionality constant, and the integral is taken between  $t = 0$  and  $t = t_p$  s.

The general trend seen in the data of Fig. 5 is supported by the proposed mechanism of ECMD represented by Eq. 1-3. Right after the additives are swept by the pad piece at a location on the wafer surface, the current density at that location is suppressed due to increased effective surface coverage of the suppressor. Then, the accelerator starts to reabsorb to restore the additive surface coverage at the swept ring with a time constant  $k$ . As the concentration of the accelerator in the plating solution is increased, reabsorption kinetics is expected to be faster, increasing  $k$  and reducing the thickness differential. Inherent in this is the assumption that the process is cyclic, and that the pad restores the swept region to the same condition at every cycle. The additive relaxation rate constant in an electrolyte with  $A = 2$  mL/L and  $S = 8$  mL/L was previously estimated to be in the range of 1.5–5 depending on the status of the copper surface in terms of prior exposure to accelerator additives.<sup>11-13</sup>

Experimental results were matched best to the model for a  $k$  value of about 1.6 s<sup>-1</sup> for wafer surfaces exposed to the plating electrolyte before the initiation of the ECMD process.<sup>11</sup> A larger effective relaxation times of around 5 s<sup>-1</sup> had to be used to obtain reasonable agreement between the experimental data and the model calculations for ECMD processes which were initiated as soon as the wafer surface touched the plating solution.<sup>12,13</sup> Because the wafer surfaces were presoaked in the plating electrolytes for 10 s in the present experiments, we assumed a  $k$  value of 1.5 s<sup>-1</sup> and plotted the dotted curve in Fig. 5 using Eq. 3 and  $t_p = 0.36$  s for a wafer rotation of 80 rpm. We assumed the value of  $k$  to be proportional to the accelerator concentration in the bath. The experimental point at  $A = 2$  mL/L was forced to match the theoretical calculation to obtain the value of the factor  $\{Bi_0\theta_{\text{pad},0}\}$ . As can be seen from Fig. 5, the general trend of the thickness differential reduction follows the theoretical prediction of our simple model. The discrepancy between the model and the experimental data points suggests that  $\theta_{\text{pad},0}$  may itself be a function of the additive concentration in the bath and, that although the mechanism of additive reabsorption to the swept surface may be represented by Eq. 3 for a given bath chemistry, its dependence on the accelerator-to-suppressor ratio may be more complex.

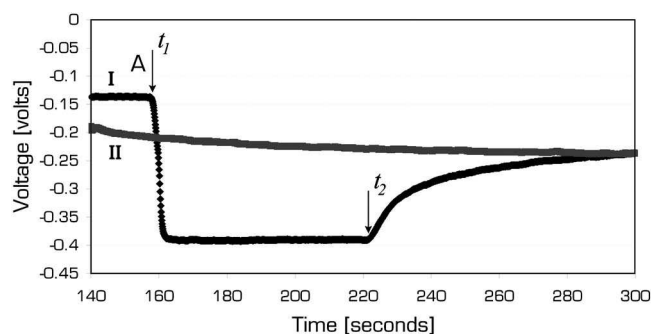


**Figure 6.** Cathode polarization data from ECD experiments in a beaker (current density of 20 mA/cm<sup>2</sup>); Scan I: 8 mL/L of suppressor added into the plating electrolyte containing 50 ppm of Cl<sup>-</sup> at time  $t_1$ , 2 mL/L of accelerator is added at time  $t_2$ . Scan II: cathode is derivitized in a solution containing 2 mL/L of accelerators, rinsed, dried, and plated in electrolyte containing 50 ppm of Cl<sup>-</sup> and 8 mL/L of suppressors. Y-axis of the graph refers to voltage with respect to the calomel reference electrode.

Scan I in Fig. 6 shows the variation of the cathodic voltage as organic additives were added into the solution where copper plating was carried out by ECD process on a 1 × 2 cm size wafer chip. The initial portion of the data corresponds to plating from the organic additive-free electrolyte containing only 50 ppm Cl<sup>-</sup> ions. At time  $t_1$ , 8 mL/L of suppressor was added into the beaker using a dropper, causing strong polarization and saturation of the voltage to a value of about -0.4 V. At time  $t_2$ , 2 mL/L of accelerator was added into the solution, causing a relatively slow depolarization of the cathode surface. As can be seen from scan I of Fig. 6, for the specific additive types and concentrations used in this work, suppressor adsorption on the fresh copper surface was rapid (within 1–2 s). The time constant observed for polarization was probably limited more by the time required to adequately mix the additive into the electrolyte than the actual adsorption onto the copper surface. In that respect, it is likely that the time constant for suppressor adsorption in our experiment was much smaller than 1 s. As for the accelerator adsorption on the already polarized copper surface, the kinetics seems to be slow, with a time constant in the order of tens of seconds.

Figure 7 shows the polarization data taken from a copper seed layer cathode which was suddenly dipped into an electrolyte containing accelerators and suppressors at concentrations of 2 and 8 mL/L, respectively. The cathode surface instantly polarizes at the time of immersion into the electrolyte ( $t = t_0$ ) and the cathode voltage rises to about -0.4 V, a value similar to the one obtained for the

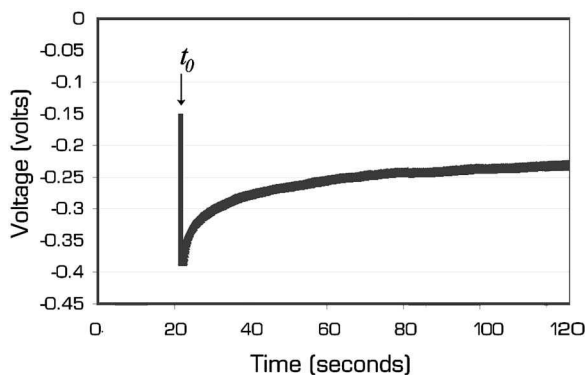


**Figure 7.** Cathode polarization data from ECD experiments in a beaker; cathode is introduced into an electrolyte with 8 mL/L of suppressors, 50 ppm of Cl<sup>-</sup>, and 2 mL/L of accelerators at time  $t_0$  and plating initiated at a current density of 20 mA/cm<sup>2</sup>. Y-axis of the graph refers to voltage with respect to the calomel reference electrode.

case of an electrolyte containing only the suppressors (Fig. 6, scan I,  $t = t_1$ ). The voltage then declines, following almost the exact trend that was seen in Fig. 6 when the accelerator was added to the suppressor containing solution. These results suggest that, when copper surface is exposed to a solution with accelerator and suppressor species, suppressors adsorb fast on the surface and the accelerators subsequently start to replace the suppressors at a much slower pace, reducing polarization.

Others have also observed that suppressor adsorption on a fresh copper surface is more rapid compared to adsorption of accelerator on a surface with already adsorbed suppressor species. For example, Akolkar and Landau found a time constant of 10 s for polyethylene glycol (PEG, with molecular weight of 3500–4000) adsorption on the copper surface under their experimental conditions, whereas injection of accelerator (C<sub>6</sub>H<sub>12</sub>N<sub>2</sub>O<sub>6</sub>S<sub>4</sub>, or SPS) into the suppressor containing electrolyte showed slow electrode depolarization with a time constant on the order of 100 s.<sup>15</sup> It was also observed that, whenever PEG and SPS species reached the electrode surface simultaneously, PEG adsorbed first, polarizing the electrode, and only later SPS started to displace the already adsorbed PEG species, thereby slowly depolarizing the electrode.<sup>15</sup>

Data in Fig. 6 and Fig. 7 show that the commercially available proprietary additives used at concentrations employed in our work were about an order of magnitude faster in terms of their adsorption kinetics compared to the additives of Ref. 15. Furthermore, in the ECMD process the copper surface is repeatedly swept by a pad which is expected to reduce the effective thickness of any boundary layer that may be forming. In Ref. 15, a boundary layer thickness,  $\delta$ , of about 18  $\mu$ m and PEG diffusion coefficient,  $D$ , of about  $5 \times 10^{-7}$  cm<sup>2</sup>/s was used to calculate the time constant for PEG adsorption,  $\tau = \delta^2/D$ , to be about 6 s. An order of magnitude reduction in the boundary layer thickness and an order of magnitude increase in the diffusion constant would yield time constants for our suppressor adsorption to be in the range of <10 ms during ECMD process. Because we have experimentally determined the  $k$  values of Eq. 2 to be in the range of 1–5 s<sup>-1</sup> the time constant for replacement of the suppressor by the accelerator in our ECMD process is on the order of 0.1–1 s, which is more than an order of magnitude smaller than what was observed for the ECD case of scan I in Fig. 6.

Based on the presented results, it would be better in an ECMD process to presoak the wafer surface in the electrolyte for a period of time before initiating plating. This way additive surface coverage at the unswept regions would be stable with a relatively high accelerator concentration before ECMD is initiated. Otherwise, if plating is started exactly at the time of entry of the wafer surface into the solution, the unswept region (cavities in the case of patterned wafers) would be rich in suppressors due to the suppressing species adsorbing rapidly on the copper surface and the accelerators taking a few more seconds to replace some of the suppressors and decreasing polarization (see Fig. 6, scan I). Therefore, especially for short depositions, planarization efficiency may be lowered due to this effect because the additive surface coverage differential between the swept and unswept surfaces would be reduced by the slow transient of the accelerator adsorption on the unswept surface. In a previous study we observed this phenomenon and mathematically accounted for the reduced planarization efficiency by increasing the effective value of  $k$  from about 1.6 to the range of 3.5–5.<sup>12</sup> It would, however, be better to eliminate this effect by presoaking the wafer surface in the process electrolyte before initiating ECMD.

The data presented above support the previously proposed MICS mechanism that may be summarized as follows. The mechanical action of the pad disturbs the steady-state surface coverage of suppressor-accelerator species. Right after the pad sweep, suppressors re-adsorb on the swept surface in a matter of a few milliseconds, while the accelerator re-adsorption takes a few hundred milliseconds. Therefore, if the wafer motion and the pad design are selected so that the time period between pad sweeps everywhere on the wafer surface is minimized (typically <300 ms), the swept areas on the wafer (top surface or the field region in the case of patterned wafers)

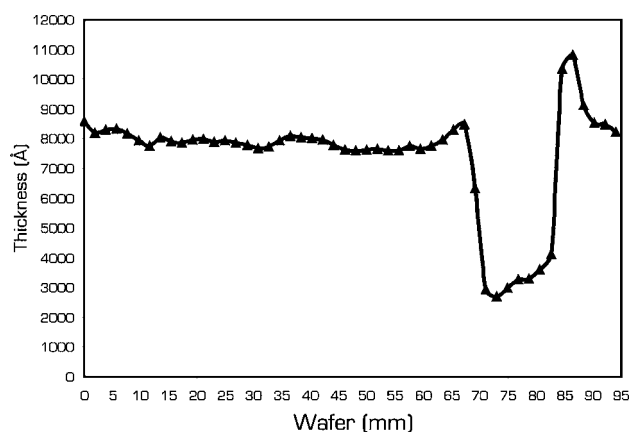


**Figure 8.** Copper layer thickness profile measured across the radius of a wafer after plating 5000 Å equivalent of copper. Wafer surface was derivatized in a solution with  $A = 2$  mL/L and plating was carried out in a solution with  $S = 8$  mL/L,  $\text{Cl}^- = 50$  ppm. Swept ring is at location between 70 and 85 mm from the wafer center.

stay adequately suppressed throughout the ECMD process, giving rise to accelerated growth on the unswept regions (cavities in patterned wafers). One way to reduce the time period between pad sweeps is to use pads in the form of multiple strips placed on the porous shaping plate.<sup>12</sup>

It was previously observed that the planarization efficiency of ECMD could be increased to over 90% by pre-exposing the copper-coated patterned wafer surface to an accelerator-rich electrolyte.<sup>12</sup> In the present work we investigated the mechanism of this efficiency enhancement by derivatizing copper seeded wafer surface in an accelerator containing DI water solution before it was plated in an electrolyte containing just suppressors. Scan II in Fig. 6 was taken from a derivatized wafer chip after it was immersed in an electrolyte with  $\text{Cl}^- = 50$  ppm and  $S = 8$  mL/L and electrodeposition was initiated. As can be seen, when electroplating started the cathode voltage was at around  $-0.2$  V and polarization increased slowly, reaching  $-0.24$  V in 160 s. This result demonstrates that, once the accelerator gets adsorbed on the copper surface, its replacement by the suppressor under ECD conditions is a slow process. Under ECMD conditions, however, our experimental results so far demonstrated that we could reduce accelerator coverage and enhance suppressor adsorption onto copper surface by sweeping the surface by a pad. Therefore, partial sweeping of derivatized blanket wafer surface should yield a large thickness differential if plating is carried out in a suppressor containing solution.

Figure 8 shows the thickness profile taken across a radius of a blanket wafer after it was first derivatized in a DI water solution with  $A = 2$  mL/L and then plated using the cell of Fig. 2 in an electrolyte containing 8 mL/L of suppressors. Then, 5000 Å equivalent of copper was deposited on the wafer. As can be seen, only about 1500–2500 Å of copper was plated within the swept ring (assuming 1200 Å thick seed layer), whereas the plated copper thickness in the unswept region was, on the average, about 6500 Å. This corresponds to up to 77% reduction in the plating current density within the swept ring. The thickness differential of 6000–7000 Å observed right at the borders of the swept and unswept wafer regions is much higher than the thickness differential given in Fig. 4, and suggests that the additive surface coverage differential in this experiment was larger. According to scan II of Fig. 6 the unswept regions of the wafer surface would stay accelerator-rich in the suppressor containing electrolyte during the 60 s plating period with cathode voltage at around  $-0.2$  V. The swept region is expected to stay highly suppressed because once the accelerator is swept off the surface by the pad, it cannot adsorb back

because there are no accelerators in the bath formulation, i.e.,  $k$  in Eq. 2 is near zero. The potential of the suppressed copper surface in Fig. 6 is about  $-0.4$  V. Therefore, the differential in surface polarization between the swept and unswept regions for the derivatized and then plated sample is expected to be large, which is in agreement with the observed large thickness differential.

### Conclusions

Mechanism of MICS was studied using a technique where a ring-shaped portion of the surface of blanket wafers was swept by small pads during electroplating of copper. Suppression of current density within the swept ring was observed and its dependence on plating bath chemistry and the preplating additive content of the wafer surface were investigated. It was found that the copper thickness differential between the swept and unswept regions of the wafer surface was a strong function of the organic additives in the plating bath. Baths containing only  $\text{Cl}^-$  ions and accelerators did not show MICS phenomenon. Electrolytes with only  $\text{Cl}^-$  ions and suppressors yielded a small degree of current suppression (about 14%) within the swept ring. Up to about 40% current density reduction was found within the swept ring in electrolytes containing both suppressors and accelerators in addition to  $\text{Cl}^-$  ions. However, as the accelerator-to-suppressor ratio was increased from about 1 to about 70, current suppression within the swept region went from 40% to about 10%. These findings are in agreement with the mechanism of MICS which was first observed during ECMD of patterned wafers and which proposes that during sweeping by the pad, accelerator surface coverage at the swept surface is reduced and suppressor coverage increases. Therefore, the unswept surface stays relatively more accelerator-rich and attracts more deposition current. In this study it was determined that the differential in suppressor surface coverage between the swept and unswept portions of the wafer could be increased by first derivatizing the wafer surface in an accelerator-containing solution and then electroplating copper in a suppressor-containing bath. This way up to 77% reduction in current density was observed within the swept ring as compared to the unswept region of the wafer.

### Acknowledgments

The authors acknowledge the contributions of their colleagues at ASM NuTool, especially of Cyprian Uzoh and Homayoun Talieh. Focused ion beam cross sections were taken by Richard Zhang.

ASM NuTool Incorporated assisted in meeting the publication costs of this article.

### References

1. P. C. Andricacos, C. Uzoh, J. O. Ducovic, J. Horkans, and H. Deligianni, *IBM J. Res. Dev.*, **42**, 567 (1998).
2. A. C. West, *J. Electrochem. Soc.*, **147**, 227 (2000).
3. J. Reid and S. Mayer, in *Proceedings Advanced Metallization Conference 1999*, p. 53, Materials Research Society, Warrendale, PA (2000).
4. D. Josell, D. Wheeler, W. H. Huber, and T. P. Moffat, *Phys. Rev. Lett.*, **87**, 016102 (2001).
5. H. Talieh, U.S. Pat. 6,176,992 (2001).
6. B. M. Basol, U.S. Pat. 6,534,116 B2 (2003).
7. B. M. Basol, C. Uzoh, H. Talieh, D. Young, P. Lindquist, T. Wang, and M. Cornejo, *Microelectron. Eng.*, **64**, 43 (2002).
8. B. M. Basol, C. Uzoh, H. Talieh, T. Wang, G. X. Guo, S. Erdemli, D. Mai, P. Lindquist, J. Bogart, M. Cornejo, M. Cornejo, and E. Basol, *Chem. Eng. Commun.*, **193**, 903 (2006).
9. T. Mourier, K. Haxaire, M. Cordeau, P. Chausse, S. DaSilva, and J. Torres, in *Proceedings Advanced Metallization Conference 2004*, p. 597, Materials Research Society, Warrendale, PA (2005).
10. I. Vos, N. Heylen, J. L. Hernandez, T. Wang, T. Truong, B. Basol, H. Sprey, and S. Vanhaelemeersch, in *Proceedings Advanced Metallization Conference 2005*, p. 539, Materials Research Society, Warrendale, PA (2006).
11. B. M. Basol, *J. Electrochem. Soc.*, **151**, C765 (2004).
12. B. M. Basol, S. Erdemli, C. Uzoh, and T. Wang, *J. Electrochem. Soc.*, **153**, C176 (2006).
13. B. M. Basol and A. C. West, *Electrochem. Solid-State Lett.*, **9**, C77 (2006).
14. T. Wang, P. Lindquist, S. Erdemli, E. Basol, R. Zhang, C. Uzoh, and B. Basol, *Thin Solid Films*, **478**, 345 (2005).
15. R. Akolkar and U. Landau, *J. Electrochem. Soc.*, **151**, C702 (2004).